Proceedings of the 1st International Workshop on Underactuated Grasping, UG2010
August 19, 2010, Montreal, Quebec, Canada

DESIGN AND FIRST EXPERIMENTS WITH A NEW UNDERACTUATED FINGER

Louis-Alain Larouche
Laboratoire de robotique
École Polytechnique de Montréal
Montréal, Québec (Canada)
H3C 3A7
louis-alain.larouche@polymtl.ca

Lionel Birglen
Laboratoire de robotique
École Polytechnique de Montréal
Montréal, Québec (Canada)
H3C 3A7
lionel.birglen@polymtl.ca

ABSTRACT

This article discusses the design and testing of a new prototype of underactuated finger obtained with a topological optimization software. Many unforeseen issues have been encountered in the developpement of this prototype and are discussed here. The aim of this paper is to give a practical look at the design of underactuated fingers and report issues that are probably common to all the designers of such fingers while being rarely, if at all, reported in the literature.

INTRODUCTION

A simple task such as grasping an apple with a human hand requires many "hardware" components: up to 19 bones, 19 muscles and 17 joints can be used to complete this task [1]. Similarly, fully actuated robotic hands such as the DLR Hand II [2], the iLimb [3] or the Robonaut Hand [4] require several motors, electrical drives and sensors in addition to complex control techniques. This makes the hardware part of the hand usually bulky and/or expensive. The underactuation technique can overcome these problems by minimizing the number of actuators required to drive the finger while maintaining good overall *grasping* performances [5]. The downside of this approach is that it does not allow *manipulation* of the objects seized: since the number of actuators has been reduced, a complex task such as reorienting an object in the hand by moving one finger after the other is impossible. However, this problem can be solved by seizing the object using another hand or by putting it on a surface, and then, regrasping it with the same hand.

Underactuation is achieved by a transmission linkage and passive elements such as mechanical limits and springs. The closing process usually goes as follow: the movement of the actuator first rotates the first phalanx joint while the relative motion of the other phalanges with respect to this first one is prevented. When a contact occurs, the closing force/torque acting on the finger is able to overcome the spring keeping the second phalanx open and thus, this phalanx begins its closing motion. This procedure is then repeated until all the phalanges are closed on the object.

The design of an underactuated finger with a shape adaptive and stable behavior is however quite complex: an impressive amount of possibilities can be looked upon and the solutions cannot usually be found intuitively. Nevertheless, the objective of this paper is to present the difficulties and the lessons learned in the physical realization and the early tests of a novel underactuated finger. The design of this finger will be introduced here, but the exact way on how the lengths and the shapes of the links are obtained will be discussed in an upcoming paper.

1 A SOFTWARE ASSISTED APPROACH

As discussed in [6], there are 3,024 two or three degree-of-freedom (DOF) possible architectures of underactuated fingers with seven or less links. To select the best architecture for a specified task, a topological optimization software has been developped by the authors [7]. Details of the software are presented in the latter reference, which currently handles only architectures with revolute joints. The input parameters of the software are: weighting values for the optimization criteria, typical objects to be seized, and lengths of the phalanges. Each architecture is then optimized separately with a genetic algorithm. The mechanical design computations handled by the software allow to establish the forces in the finger, the generated contact forces, the actuator position of a specified grasp, and the (non-straight) shape of the links of the finger if required to eliminate interferences. The criteria evaluated are the stability of the finger, compactness,

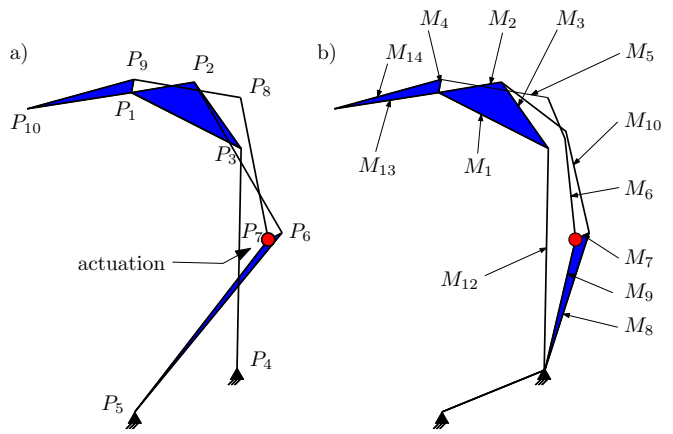

Figure 1. Linkage selected for prototyping (referred to as $D7812-7$): a) kinematics, b) with non-straight links.

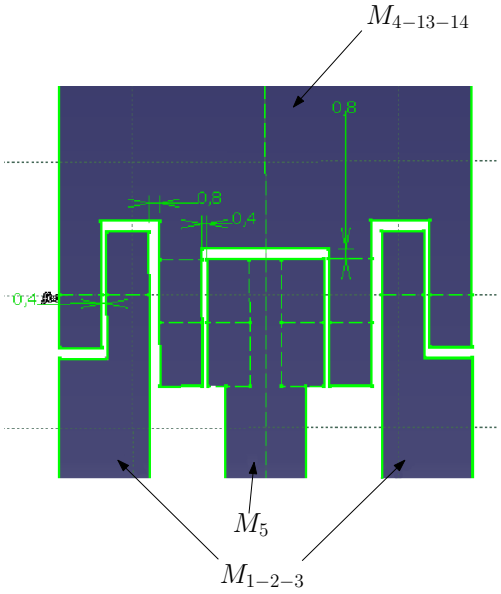

Figure 2. Clearances around the distal phalanx joint.

contact force isotropy, grasp stiffness and size of the workspace. Once each architecture has been optimized and evaluated, their respective scores are compared one against the other to select the best overall architecture. The finger discussed in this paper is the result of such an optimization procedure. With the current software (MATLAB^{TM}) and hardware (Workstation with Intel Xeon^{TM}processor), the vectorized software runs at approx. 100 evaluations per second and one entire optimization process takes around 150 h of computing time.

2 MECHANICAL DESIGN

Following the first test of the software, the mechanism presented in Fig. 1 has been obtained. The lefthand side drawing presents the original kinematics of the finger while the righthand side illustrates this design with non-straight links thus eliminating mechanical interferences. Revolute joints are identified by P_i and binary links by M_i. Other links referred to as M_{i-j-k} are ternary links constituted by the three binary links M_i, M_j and M_k. Minor changes have been made in the software since then, thus making this design actually non-optimal with the latest software version. Yet, it is representative of the capability of the software and offers a glimpse to new designs of underactuated fingers.

2.1 Rapid prototyping tolerances

Since this prototype was to be built with a ZCorp Z450 3D printer, a few test parts have been printed to check the accuracy of the printer. These parts have been measured with a numerical vernier. Following the cyanoacrylate impregnation, the parts are oversized between 0.07 mm and 0.10 mm per face for directions perpendicular to the construction layers, and between 0.10 mm and 0.18 mm per face for the directions parallel to the layers. Therefore, a maximal oversize of 0.2 mm per face is considered in the mechanical design of the parts. By following this guideline, two functional faces should theoretically be apart of at least 0.4 mm to prevent any jamming in the assembly. As a safety margin, the clearance between two non-functional faces has been selected to 0.8 mm as illustrated in Fig. 2.

2.2 Revolute joints

The revolute joints in the prototype are made with brass shafts in nylon sleeves (glued to the printed links). The parts are modeled with a hole of 4.760 mm in which the $\frac{3}{16} \pm 0.005$ in. (4.76 ± 0.13 mm) sleeves are located. Due to the oversizing in the printing process, the holes are manually drilled with a $\frac{3}{16}$in. drill bit giving then a smooth surface finish and proper tolerances. The sleeves (McMaster part # 94639A702) are then fitted in these holes. The brass shafts are made from 2.91 mm (0.115") rods (McMaster part # 8859K156) trimmed and sanded to 2.89$\pm$0.01 mm. The use of standard nylon sleeves with modified diameter polished brass shafts allows the joints to have almost no clearance with very low friction.

2.3 Actuator assembly and safety features

In Fig. 3, the motor driving the finger (Maxon RE10 with a GP10A 16:1 gearhead) is presented. It is located inside link M_{7-8-9} which allows to save space under and around the finger. Therefore, the motor axis and its attached reference frame are moving as the finger is closing. The motor is pushed through a cylinder bore in link M_{7-8-9} and screwed in a thrust washer illustrated in the figure. The thrust washer has been trimmed

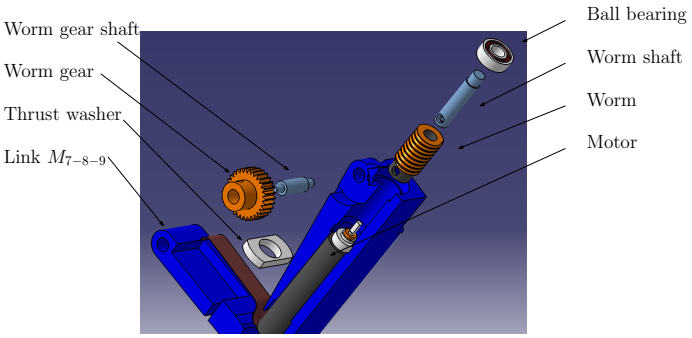

Figure 3. Exposed view of the actuator components (link M_{7-8-9} is cut for illustration purposes).

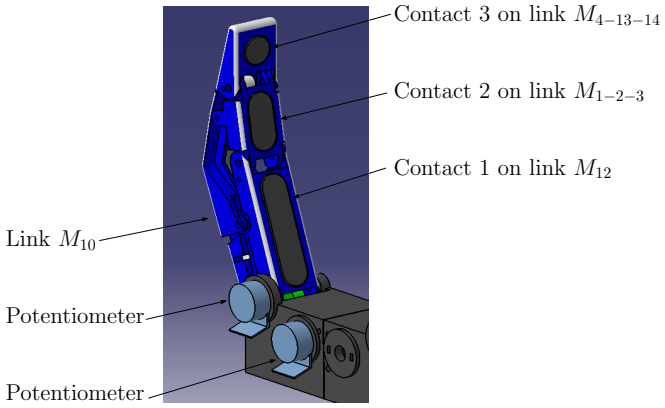

Figure 4. Isometric view of the finger in the initial position.

and threaded first and then, slided in a slot and screwed to the motor. A worm gear (SDP/SI # S1D94Z-P048SS) is slided on a steel shaft, and then assembled on the gearhead output shaft. A very long pressure screw is used to transmit power from the gearhead shaft to the worm through a hole in the steel shaft. On the other end of the steel shaft, the diameter is reduced so that a ball bearing can be press fit on it. This 11 mm ball bearing is glued on a shoulder in link M_{7-8-9}.

At approximately 400 CAN$, the motor assembly (motor+gearhead+encoder) is by far the most expensive part of this finger. It is actually also the most fragile part because of the gearhead shaft. Indeed, while one may think that the parts built using rapid prototyping might be weak, they were not the main concern of this design. Our main issue was that the maximal permissible axial load on the gearhead shaft is only 5 N. Thus, this actuator assembly includes two safety features to prevent damages on this axis. First, the closing motion of the finger is designed to generate only compression between the bearing and the shoulder it is resting on. By having a close fit between the steel shaft of the worm and the ball bearing, and a pressure screw between the worm and its shaft, the worm cannot significantly move towards the gearhead. Second, if the finger receives an external impact forcing it to close, traction will arise between the bearing and its the shoulder. If the impact force is big enough, the glue holding the bearing will break and eject it from link M_{7-8-9}: therefore, the fragile axis should not absorb most of the impact. It should be noted that these two features are only possible in practice if the pressure screw is not overtightened on the gearhead.

2.4 Instrumentation

Since this is a prototype, it has been decided to place position and force sensors in the finger as illustrated in Fig. 4. Note that these sensors are not necessary to the operation of the finger. For measuring the position of the finger, two additional sensors to the encoder of the motor must be placed since the finger has three DOF. The pose, i.e. the three angles of the phalanges, is computed from this data with the technique described in [7]. Potentiometers have been selected for this purpose and are attached to revolute joints on links M_{7-8-9} and M_{12}.

Five $1/2$ in. force sensing resistors (FSR) from Interlink are used to measure the contact forces. Two sensors are placed on the proximal and intermediate phalanges while, due to their sizes, only one is located on the distal phalanx. They have been integrated with their electrical connectors in the most compact way possible. Each FSR is glued on both sides to a 0.5 mm protrusion built in the part. As seen in Fig. 5a), a hole is made in link M_{12} for the wires of the sensors and to give enough space to the worm gear when the finger is closing. Inside the second phalanx, the wires of the sensor are going through a small slot and are corkscrewed to their connectors (Fig. 5b). This twisting allows the cable to clear the center of the phalanx where link M_5 is moving. The core of the distal phalanx is hollow, as seen in Fig. 5c), in order for the connector and the sensor to be attached together.

2.5 Springs and cables

Two springs are required to fully constrain the finger since one actuator drives it. As seen in Fig. 6 these springs have been located in the base. They are hooked to the phalanges by nylon wires properly routed through the finger. Since the wires change direction a few times on their way to the phalanges, brass pivots are used as pulleys. The second phalanx cable passes by the $M_{12} - base$ axis, goes under axis D (see Fig. 5b)), over a corner of link M_{1-2-3}, and is attached to the axis between $M_{1-2-3} - M_{10}$. The distal phalanx cable also passes by the $M_{12} - base$ axis, goes under axis D, over the axes between $M_{1-2-3} - M_{12}$, over axis $M_{1-2-3} - M_{10}$, and is hooked at axis $M_5 - M_{4-13-14}$. The stiffness of the springs has been measured to $136 \pm 10\%$ Nm.

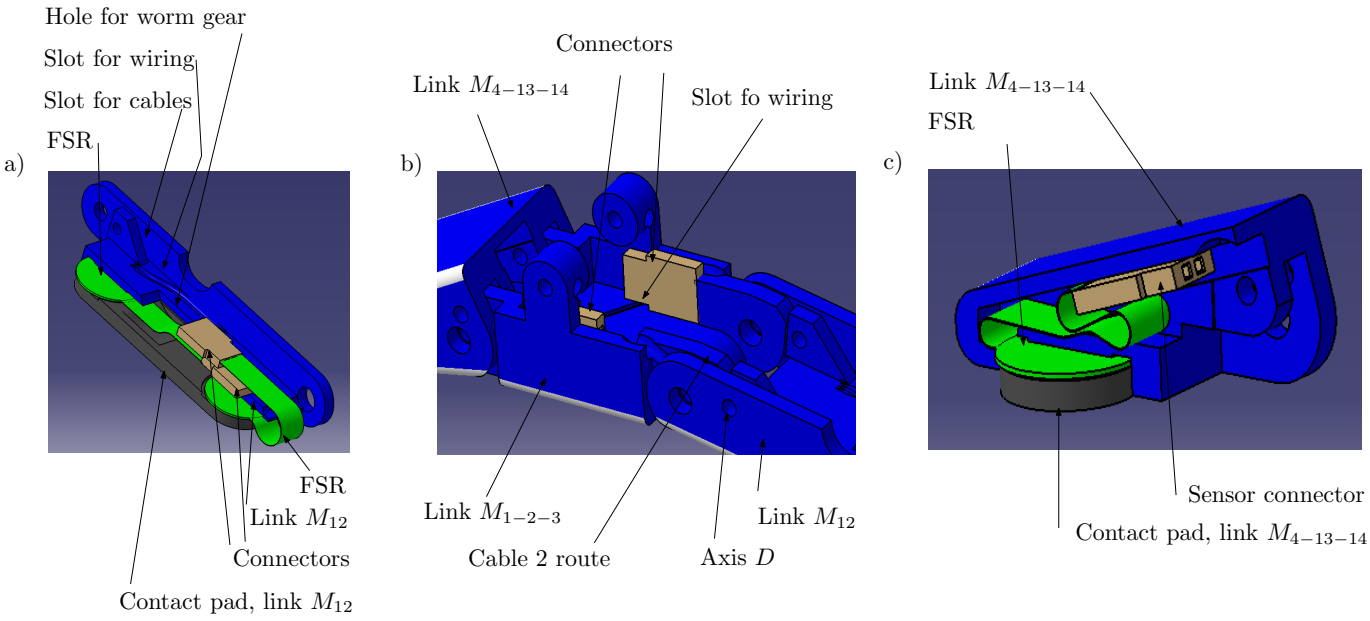

Figure 5. FSR sensors on the: a) proximal, b) intermediate, and c) distal phalanx.

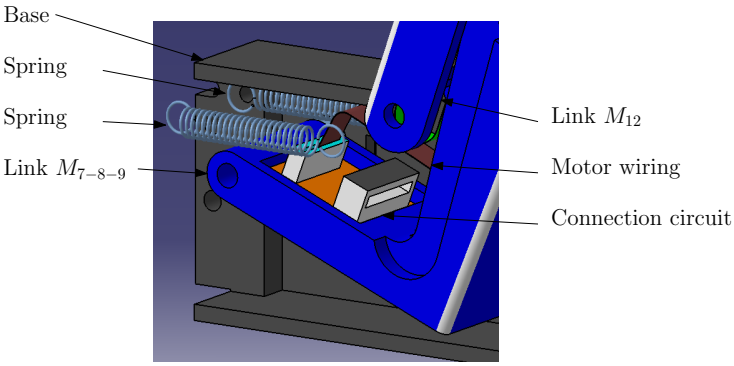

Figure 6. Isometric view of the finger palm: springs and electrical connectors.

3 TESTING

3.1 Worm gear issues

A worm gear has been selected to transmit the actuator torque to the finger since it is non-backdriveable. This is a very desirable property in the actuation of underactuated fingers since it allows for maintaining a grasp in the case of a power failure and eliminates problems such as non force-closure arising when two opposite fingers are seizing an object [8]. At first, the design distance between the axes of the worm gear and the worm itself was the sum of the two pressure diameter, thus having no clearance between the two parts. Once built with rapid prototyping and put together, such assembly did not move at all even without any load on the finger. The source of the problem was determined to be the distance between the two pressure diameters: a clearance was required. A test part with a distance of 0.50 mm has been printed on the 3D printer. As seen in Fig. 7, this test part is a reproduction of the actuator assembly introduced earlier. Link M_6 has been installed on the worm gear, just as in the finger, and loads have been applied at the end of this link. With a maximal continuous torque output of 1.54 mNm, a 16:1 gearhead, and a 20:1 worm gear assembly, a maximal theorical torque of 0.49 Nm was expected. However, the largest torque attainable by the system in practice was around 0.11 Nm. The discrepancy between these numbers are mainly due to the friction caused by the lack of precision in the positioning of the parts and the gearhead efficiency. Hence, while a worm gear is very interesting to obtain a non-backdriveable finger and is compact, a particular attention should be paid to the clearance of this part of the mechanism. Proper lubrication is also a good idea. It should be noted that even if properly installed, worm gears generally have a low efficiency, and a loss of actuation power must be expected.

3.2 Closing sequence issues

Once the new link M_{7-8-9} was ready, the finger was put together for the first actual experiments. When closed, the finger was able to give a stable and satisfying grasp on many randomly placed and shaped objects. However, during the closing sequence, the third phalanx was sometimes moving before the second one. This problem has been addressed by increasing the spring force acting on the distal phalanx. The final routing of the

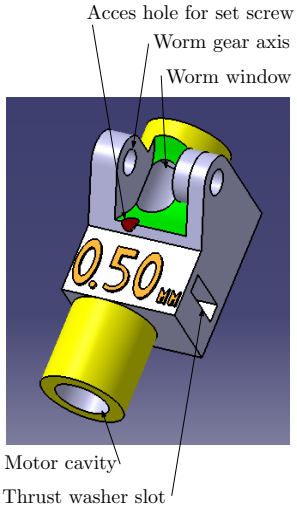

Figure 7. Test part for the motor-worm gear assembly.

cable can be seen in Fig. 5 b): a small hole (not illustrated) has been drilled through the phalanx where the arrow $M_{4-13-14}$ ends. Using this technique, the resulting opening torque created by this spring is increased and a proper closing process is obtained.

3.3 Force and torque issues

Another issue the authors faced was that when closing, the last phalanx appeared weak: it often needed a few gentle taps to help it closing. Originally, the finger was supposed to be 33% smaller than the current prototype (final lengths of the proximal/intermediate/distal phalanges are 8.33/4.66/4 cm). However, during the design process, it has been discovered that this would be impossible since the 20:1 worm gear would interfere with the contact pad of the proximal phalanx. By multiplying every dimensions by 1.5, this mechanical interference was avoided by allowing for a hole to be placed in link M_{12} (see Fig. 5a)). Unfortunately, this reduced to ratio of motor torque to finger size.

Once it was decided that the motor gearbox ratio should be increased, the action of this new motor was simulated. Two conditions were decided to be checked during the complete closing process to test if the motor was indeed satisfactory. Beforehand, a variable c representing the closing step is introduced: at 0 the finger is fully open, and at its maximal value the finger is fully closed. The actual maximal value of c has no importance since it is an adimensional variable. The first condition was that the amount of actuator torque times its displacement (i.e. actuator input work) should be larger than the variation of the potential energy stored in the springs, i.e.

$$T_a \Delta\theta_a(c) > \Delta E_r c \quad \text{with} \quad (1)$$

$$\Delta E_r c = \sum_{i=1}^{2} \left[\frac{1}{2} K (x_i(c) - x_i(c_{rest}))^2 - \frac{1}{2} K (x_i(0) - x_i(c_{rest}))^2 \right] \quad (2)$$

$$\text{and } \Delta\theta_a(c) = \theta_a(c) - \theta_a(0) \quad (3)$$

where T_a is the actuation torque, θ_a is the actuator angle, $\theta_a(0)$ is the actuator angle when the finger is fully open, K is the stiffness of both springs, $x_i(c)$ is the deflection angle of the i^{th} spring which has a resting position noted $x_i(c_{rest})$. If this relation is not always true, it is physically impossible for the finger to close due to a lack of energy provided by the actuator. This equation introduces an inequality since it does not accounts for the stored kinetic energy: this energy could be converted back into potential energy when the finger is slowing down. The actuator torque is considered constant during the closing motion.

The second condition is that, at any point, the maximal actuation torque around the joint of the phalanx in motion should be greater than the opposed torque caused by the deformation of the springs, i.e.

$$T_a \frac{\Delta\theta_a(c)}{d\theta_i(c)} > \frac{dE_r(c)}{d\theta_i(c)} \quad (4)$$

$$\text{with } E_r c = \sum_{i=1}^{2} \frac{1}{2} K (x_i(c) - x_i(c_{rest}))^2 \quad (5)$$

$$\text{and } \Delta\theta_a(c) = \theta_a(c) - \theta_a(0) \quad (6)$$

If this relation is not always true, the finger will probably not close due to a lack of torque. However, the finger could still theoretically be in a closing motion because it would have stored enough kinetic energy, as mentioned earlier. Here, θ_i represents the relative angle of the i^{th} phalanx joint currently in motion with respect to the previous phalanx (or base in the case of the proximal phalanx) and E_r is the potential energy stored in the springs.

In Fig. 8, the finger is grasping an object which causes a near-singularity right after phalanx joint 2 is set in motion. Figure 8c) illustrates this problematic pose where it can clearly be seen that this the near-singular aspect of the linkage is not obvious. In Fig. 8a), it is shown that the curve slope of the input power (i.e. the relative motion of the actuator to the phalanx for a constant torque) is slightly negative: this implies the actuator should reverse its motion to close the finger. Also, at the end of the distal phalanx closing motion, as illustrated in Fig. 8b) the torque generated by the motor is not strong enough to close the phalanx. Since this figure represents the case with a 16:1 gearhead, the actuating torque T_a = 0.0954 Nm is obtained by $T_a = C_{mmct} R_{gh} R_{wg} E_{wg}$ where C_{mmct} = 1.54 mNm is the motor

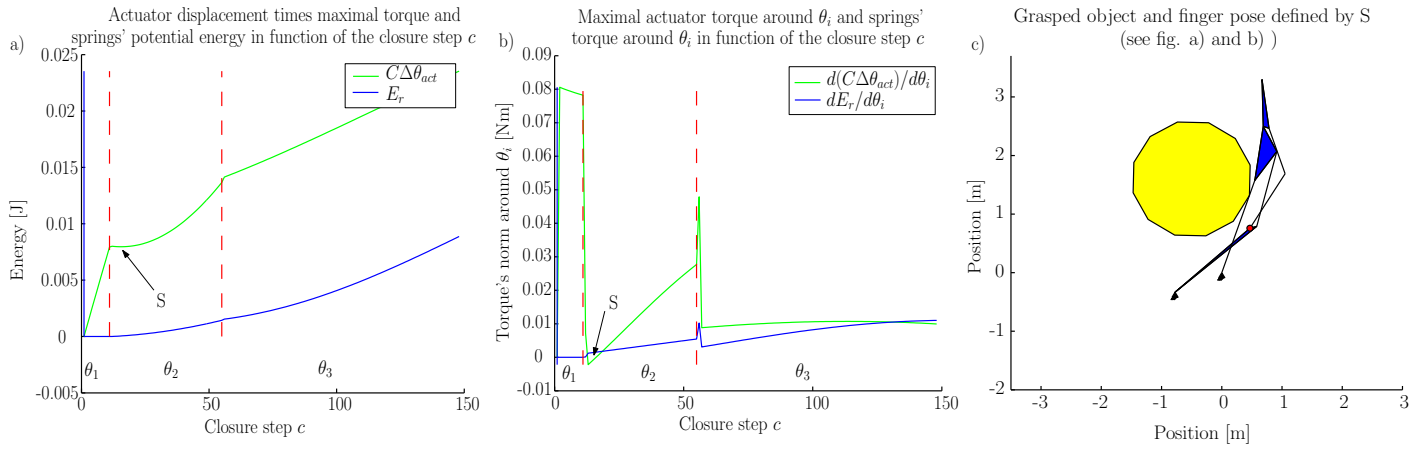

Figure 8. Issues during the closing motion of the finger grasping an object with a 16:1 gearhead (C=0.0954 Nm): a) energy, b) torque, c) S pose.

maximal continuous torque, R_{gh} = 16 is the gearhead ratio, R_{wg} = 20 is the worm gear ratio and E_{wg} = 0.2 is the overall efficiency of the actuator, gearhead and worm gear as measured in Section 3.1.

CONCLUSION

As discussed in this paper, the prototype introduced here has been designed with a software assisted approach. Close to 150 h of computing time were required to obtain this architecture. This architecture features good overall stability, force isotropy, grasp stiffness, a large workspace, and a low encumbrance. Several links in the transmission mechanism are non-straight to avoid mechanical interferences, and the motor is installed in one of these links.

The links of this prototype have been made with a 3D printer. They have been modified to reduce tolerances and are held together with revolute joints made from nylon sleeves and polished brass axes. The finger has safety features to prevent damages to the motor gearhead caused by accidental impacts, and it is fully instrumented with position and force sensors. A system of cables are linking the springs located in the palm to the phalanges. A non backdriveable worm gear transmits the actuator torque to the finger.

Since the objective of this paper is to present the lessons learned in the development of the prototype, the many issues encountered during the testing are reminded here: first, friction was experienced in the worm gear due to a lack of proper clearance in addition to an already low efficiency. Second, the spring torque on the third phalanx was insufficient and led to a modified routing of the associated cable to achieve the proper closing sequence. Finally, a near-singularity has been discovered in the linkage during the grasping of some objects. This was a major concern and proves that with new prototypes of underactuated fingers, not only the property of the latter when contacting objects must be optimized but also its grasping sequence should be carefully analyzed.

For the workshop, the authors will present a new version of this finger with a higher ratio gearbox (illustrated in Fig. 9). The lessons learned here will also be implemented in the optimization software. We made mistakes in the design of this new prototype but we are learning a lot from them and first results are *still* encouraging.

Figure 9. Prototype.

ACKNOWLEDGMENT

The financial support of the National Sciences and Engineering Research Council of Canada (NSERC), the Canadian Foundation for Innovation (CFI) and the Fonds Québécois de la Recherche sur la Nature et les Technologies (FQRNT) is gracefully acknowledged.

REFERENCES

[1] Tubiana, R., Thomine, J.-M., and Mackin, E., 1998. *Examination of the Hand and Wrist*, 2nd editio ed. Taylor & Francis.

[2] J. Butterfass M. Grebenstein, H. L., and Hirzinger, G., 2001. "DLR-Hand II: Next Generation of a Dextrous Robot Hand". In Proceedings of the 2001 IEEE International Conference on Robotics & Automation, Vol. 1, pp. 109–114.

[3] Bionics, T., 2009. "The i-LIMB hand prosthesis". *http://www.touchbionics.com/*.

[4] Diftler, M. A., Ambrose, R. O., Tyree, K. S., and Goza, S. M., 2004. "A Mobile Autonomous Humanoid Assistant". In 4th IEEE/RAS International Conference on Humanoid Robots, pp. pp.˜133—-48.

[5] Birglen, L., Laliberté, T., and Gosselin, C., 2008. *Underactuated Robotic Hands*. Springer Tracts in Advanced Robotics.

[6] Birglen, L., 2009. "Type Synthesis of Linkage-Driven Self-Adaptive Fingers". *Journal of Mechanisms and Robotics,* **1**(2).

[7] Larouche, L.-A., 2009. "Logiciel de conception de doigts sous-actionnés". Mémoire de maîtrise, École Polytechnique de Montréal.

[8] Bégoc, V., Durand, C., Krut, S., Dombre, E., and Pierrot, F., 2006. "On the form-closure capability of robotic underactuated hands". *on Control, Automation, Robotics*, pp. 1–8.